PERGAMON

International Journal of Solids and Structures 38 (2001) 9111–9131

INTERNATIONAL JOURNAL OF SOLIDS and STRUCTURES

www.elsevier.com/locate/ijsolstr

Practical advanced analysis for semi-rigid space frames

Seung-Eock Kim [a,*], Se-Hyu Choi [b]

[a] *Department of Civil and Environmental Engineering, Sejong University, 98 Koonja-dong, Kwangjin-ku, Seoul 143-747, South Korea*
[b] *Construction Technology Research Institute, Sejong University, 98 Koonja-dong, Kwangjin-ku, Seoul 143-747, South Korea*

Received 15 November 2000; in revised form 15 May 2001

Abstract

A practical advanced analysis of semi-rigid space frame is developed. Herein, the nonlinear behavior of beam-to-column connections is discussed, and practical modeling of these connections is introduced. The proposed analysis can predict accurately the combined nonlinear effects of connection, geometry, and material on the behavior and strength of semi-rigid frames. Kishi–Chen power model is used to describe the nonlinear behavior of semi-rigid connections. Stability functions are used to capture second-order effects associated with P-δ and P-Δ effects. The column research council tangent modulus and a parabolic function for gradual yielding are used to represent material nonlinearity. The load–displacements predicted by the proposed analysis compare well with those available experiments. A case study has been performed for a four story semi-rigid frame.

Keywords: Advanced analysis; Semi-rigid connection; Geometric nonlinearity; Material nonlinearity; Steel frame

1. Introduction

Conventional analysis of steel frame structures is usually carried out under the assumption that the beam-to-column connections are either fully rigid or ideally pinned. However, most connections used in current practice are semi-rigid type whose behavior lies between these two extreme cases. In the AISC-LRFD Specification (AISC, 1993), two types of constructions are designated: type fully restrained construction; and type partially restrained construction. The LRFD Specification permits the evaluation of the flexibility of connections by rational means when the flexibility of connections is accounted for in the analysis and design of frames.

The semi-rigid connections influence the moment distribution in beams and columns as well as the drift (P-Δ effect) of the frame. One way to account for all these effects in semi-rigid frame design is through the use of a direct second-order inelastic frame analysis known as ''advanced analysis''. Advanced analysis indicates a method that can sufficiently capture the limit state strength and stability of a structural system and its individual members so that separate member capacity checks are not required. Since the power of

* Corresponding author. Tel.: +82-2-3408-3391; fax: +82-2-3408-3332.
E-mail address: sekim@sejong.ac.kr (S.-E. Kim).

0020-7683/01/$ - see front matter
PII: S0020-7683(01)00141-X

personal computers and engineering workstations is rapidly increasing, it is feasible to employ advanced analysis techniques directly in engineering design office.

During the past 20 years, research efforts have been devoted to the development and validation of several advanced analysis methods. The advanced analysis methods may be classified into two categories: (1) plastic-zone method; and (2) plastic hinge method. Whereas the plastic-zone solution is known as the "exact solution", but cannot be used for practical design purposes (Chen and Toma, 1994). This is because the method is too intensive in computation and costly due to its complexity.

Advanced analyses for two-dimensional steel frame with rigid and semi-rigid connection were developed by Lui and Chen (1986), Al-Mashary and Chen (1991), Kishi and Chen (1986, 1990), Liew (1992), Kim and Chen (1996a,b), and Barsan and Chiorean (1999). Second-order inelastic analyses for the space steel frames with rigid connections were developed by Orbison (1982), Prakash and Powell (1993), and Liew and Tang (1998). Orbison's method is an elastic–plastic hinge analysis without considering shear deformations. The material nonlinearity is considered by the tangent modulus E_t and the geometric nonlinearity is by a geometric stiffness matrix. Orbison's method, however, underestimates the yielding strength up to 7% in stocky members subjected to axial force only. DRAIN-3DX developed by Prakash and Powell (1993) is a modified version of plastic hinge methods. The material nonlinearity is considered by the stress–strain relationship of the fibers in a section. The geometric nonlinearity caused by axial force is considered by the use of the geometric stiffness matrix, but the nonlinearity caused by the interaction between the axial force and the bending moment is not considered. This method overestimates the strength and stiffness of the member subjected to significant axial force. Liew and Tang's method is a refined plastic hinge analysis. The effect of residual stresses is taken into account in conventional beam-column finite element modeling. Nonlinear material behavior is taken into account by calibration of inelastic parameters describing the yield and bounding surfaces. Liew and Tang's method, however, underestimates the yielding strength up to 7% in stocky member subjected to axial force only. The analysis for the space steel frames with semi-rigid connections was developed by Shakourzadeh et al. (1999). The work proposed by Shakourzadeh et al. was on modeling of connections in the analysis of thin-walled space frames.

We shall develop a practical advanced analysis using plastic-hinge concept for semi-rigid space frames. This paper combines nonlinear behavior of framed members and that of semi-rigid connection. The analysis is equivalent to the plastic-zone analysis in its accuracy but is much simpler than the plastic-zone analysis. Lateral torsional buckling of members is assumed to be prevented by adequate lateral braces. Also a compact W-section is assumed so that the section can develop full plastic moment capacity without local buckling.

2. Behavior of semi-rigid frames

The important attributes that affect the behavior of semi-rigid steel frame structures may be grouped into three categories: connection, geometric, and material nonlinearities. The connection nonlinearity indicates the nonlinear moment–rotation relationship of semi-rigid connections. The geometric nonlinearity includes second-order effects associated with the P-δ and P-Δ effects and geometric imperfections. The material nonlinearity includes gradual yielding associated with the influence of residual stresses on flexure behavior.

2.1. Nonlinear behavior of connections

The forces transmitted through beam-column connections consist of axial force, shearing force, bending moment, and torsion. The effect of axial force, shearing force, and torsion is negligible since their deformations are small compared with the rotational deformation of connections. The deformation behavior of

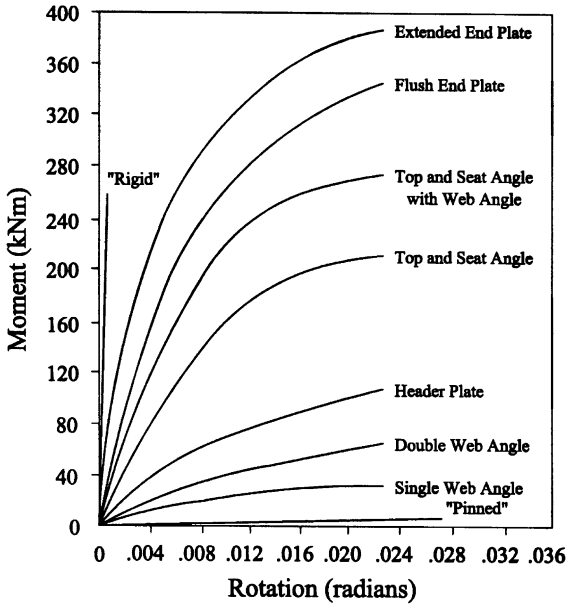

Fig. 1. Schematic moment–rotation curves of various semi-rigid connections.

a connection may be customarily described by moment–rotation relationship, and its typical behavior is nonlinear. The schematic moment–rotation curves of commonly used semi-rigid connections are shown in Fig. 1. It may be observed that a relatively flexible connection has a smaller ultimate moment capacity and a larger rotation, and vice versa. Herein, Kishi–Chen power model shall be adopted to describe the moment–rotation relationship of semi-rigid connections (Kishi and Chen, 1990).

If the direction of incremental moment applied to a connection is reversed, the connection will unload with the initial slope of the moment–rotation curve. This loading and unloading behaviors of connections can be adequately accounted for by the use of tangent stiffness and initial stiffness, respectively (Chen and Lui, 1991). Herein, these stiffnesses shall be obtained by simply differentiating Kishi–Chen power model equation.

2.2. Geometric nonlinearity

The bending moments in a beam-column consist of two types: primary bending moment; and secondary bending moment. Primary bending moments are caused by applied end moments and/or transverse loads on members. Secondary bending moments are from axial compressive force acting through the lateral displacements of a member. The secondary bending moments include the P-δ and P-Δ moments. Herein, stability functions are used for each member to capture these second-order effects in a direct manner.

2.3. Material nonlinearity

Residual stresses result in a gradual axial stiffness degradation. The fibers that have the highest compressive residual stress will yield first under compressive force, followed by the fibers with a lower value of compressive residual stress. Due to this spread of yielding or plasticity, the axial and bending stiffnesses of a

column segment are degraded gradually along the length of a member. This stiffness degradation effect will be accounted for later by the tangent modulus concept (Liew, 1992).

When a wide flange section is subjected to pure bending, the moment-curvature relationship of a section has a smooth transition from elastic to fully plastic. This is because the section yields gradually from extreme fibers which have higher stresses than interior fibers. The gradual yielding effect leads to the concept of a hardening plastic hinge which may be represented simply by a parabolic stiffness reduction function of a plastic hinge (Liew, 1992). This will be described later.

3. Practical connection modeling

The connection behavior is represented by its moment–rotation relationship. Extensive experimental works on connections have been performed, and a large body of moment–rotation data has been collected (Goverdhan, 1983; Nethercot, 1985; Kishi and Chen, 1986; Chen and Kishi, 1989). Using these abundant database, researchers have developed several connection models including: linear; polynomial; B-spline; power; and exponential models. Herein, the three-parameter power model proposed by Kishi and Chen (1990) is adopted. The Kishi–Chen power model contains three parameters: initial connection stiffness R_{ki}, ultimate connection moment capacity M_u, and shape parameter n. The power model may be written as (Fig. 2):

$$m = \frac{\theta}{(1+\theta^n)^{1/n}} \qquad \text{for} \quad \theta > 0, \ \ m > 0 \tag{1}$$

where $m = M/M_u$, $\theta = \theta_r/\theta_0$, $\theta_0 =$ reference plastic rotation, M_u/R_{ki}, $M_u =$ ultimate moment capacity of the connection, $R_{ki} =$ initial connection stiffness, and $n =$ shape parameter. When the connection is loaded, the connection tangent stiffness (R_{kt}) at an arbitrary rotation θ_r can be derived by simply differentiating Eq. (1) as:

$$R_{kt} = \frac{\mathrm{d}M}{\mathrm{d}|\theta_r|} = \frac{M_u}{\theta_0(1+\theta^n)^{1+1/n}} \tag{2}$$

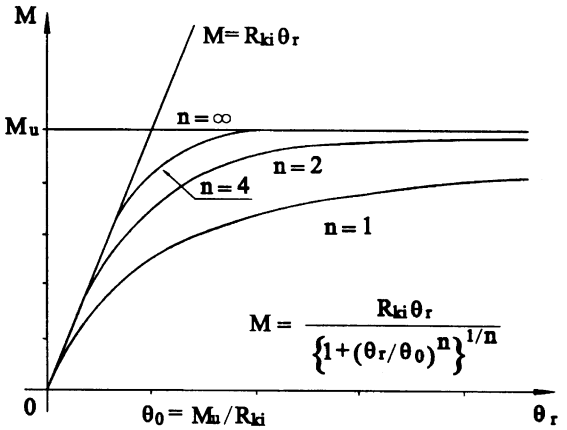

Fig. 2. Moment–rotation behavior of three-parameter model.

When the connection is unloaded, the tangent stiffness is equal to the initial stiffness as:

$$R_{kt} = \frac{\mathrm{d}M}{\mathrm{d}|\theta_r|} = \frac{M_u}{\theta_0} = R_{ki} \tag{3}$$

It is observed that a small value of the power index n makes a smooth transition curve from the initial stiffness R_{kt} to the ultimate moment M_u. On the contrary, a large value of the index n makes the transition more abruptly. In the extreme case, when n is infinity, the curve becomes a bilinear line consisting of the initial stiffness R_{ki} and the ultimate moment capacity M_u.

An important task for practical use of the power model is to determine the three parameters for a given connection configuration. Herein, the practical procedures for determining the three parameters are presented for the following four types of connections with angels: single/double web-angle connections; and top and seat angle with/without double web-angle connections.

The values of R_{ki} and M_u can be determined by a simple mechanical procedure with an assumed failure mechanism (Kishi and Chen, 1990). For single/double web-angle connections shown in Fig. 3, the initial connection stiffness and the ultimate moment capacity are given by:

$$R_{ki} = G\frac{t_a^3}{3}\frac{\alpha\cosh(\alpha\beta)}{(\alpha\beta)\cosh(\alpha\beta) - \sinh(\alpha\beta)} \tag{4}$$

$$M_u = \frac{2V_{pu} + V_0}{6} d_a^2 \tag{5}$$

where G = shear moduli, t_a = thickness of web-angle, $\alpha = 4.2962$ when Poisson's ratio is 0.3, $\beta = g_1/d_a$, d_a = height of web-angle, g_1 = distance from the fixed support line to free edge line as shown Fig. 3(a), V_{pu} = minimum value of V_{py}, V_0 = maximum value of V_{py}, and V_{py} = plastic shear force per unit length.

For the top and seat angle connections shown in Fig. 4, the initial connection stiffness and the ultimate moment capacity are given by:

$$R_{ki} = \frac{3EI}{1 + (0.78t_t^2/g_1^2)}\frac{d_1^2}{g_1^3} \tag{6}$$

$$M_u = M_{0s} + M_p + V_p d_2 \tag{7}$$

where EI = bending stiffness of angle's leg adjacent to column face, $g_1 = g_t - (D/2) - (t_t/2)$, g_t = gage distance from top angle's heel to center of fastener holes in leg adjacent to column face, $D = d_b$ for rivet fastener, $D = W$ for bolt fastener, d_b = the diameter of the fastener, W = the diameter of the nut, t_t = thickness of top angle, d_1 = distance between centers of horizontal legs of top and bottom angles $(= d + (t_t/2) + (t_s/2))$, t_s = thickness of the bottom angle, d = total depth of the beam section, M_{0s} = plastic moment capacity at point C, M_p = plastic moment capacity at point H_2 of top angle, V_p = shear force, $d_2 = d + (t_s/2) + k$, and k = distance from the top angle's heel to the toe of the fillet.

For top and seat angle connections with double web-angles shown in Fig. 5, the initial connection stiffness and the ultimate moment capacity are given by:

$$R_{ki} = \frac{M}{\theta_r} = \frac{3EI_t d_1^2}{g_1(g_1^2 + 0.78t_t^2)} + \frac{6EI_a d_3^2}{g_3(g_3^2 + 0.78t_a^2)} \tag{8}$$

$$M_u = M_{0s} + M_{pt} + V_{pt}d_2 + 2V_{pa}d_4 \tag{9}$$

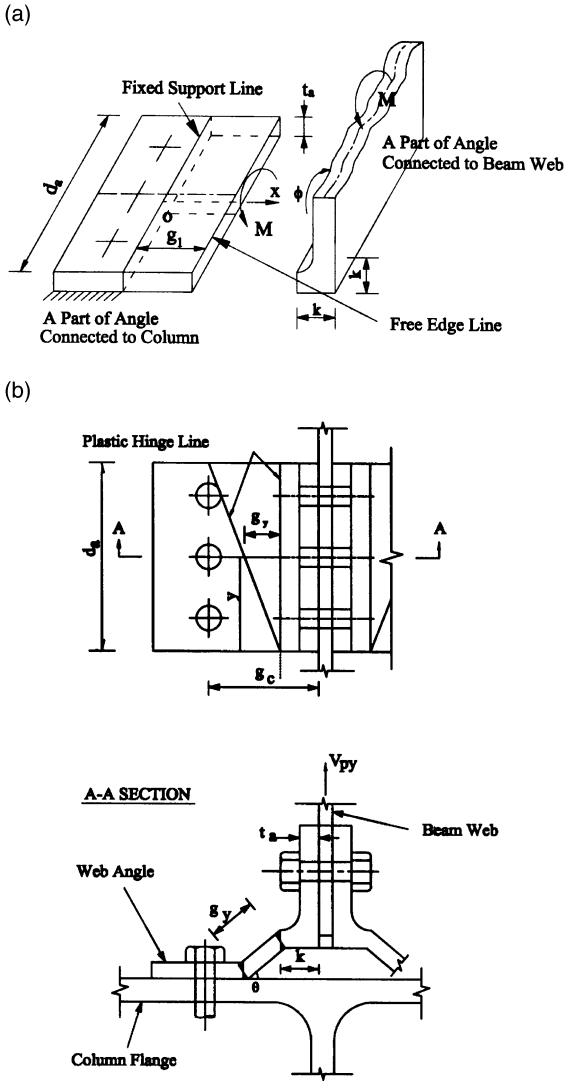

Fig. 3. Web-angle connection. (a) Moderate thick plate modeling and (b) mechanism at ultimate condition.

where EI_t, EI_a = bending stiffness of legs adjacent to column face of top angle and web-angle, $g_3 = g_c - W/2 - t_a/2$, W = diameter of nut, t_a = thickness of top angle, M_{pt} = ultimate moment capacity of top angle, V_{pt} = shearing force acting on plastic hinges, V_{pa} = resulting plastic shear force, $d_4 = (2V_{pu} + V_{0a})d_a/3(V_{pu} + V_{0a}) + l_l + t_s/2$, V_{pu} = shearing force at upper edge of web-angle, V_{0a} = shearing force at lower edge of web-angle, and l_l = distance from bottom edge of web-angle to compression flange of beam.

As for the shape parameter n, the equations developed by Kishi et al. (1991) are implemented here. Using a statistical technique for n values, empirical equations of n are determined as a linear function of $\log_{10}\theta_0$ shown in Table 1.

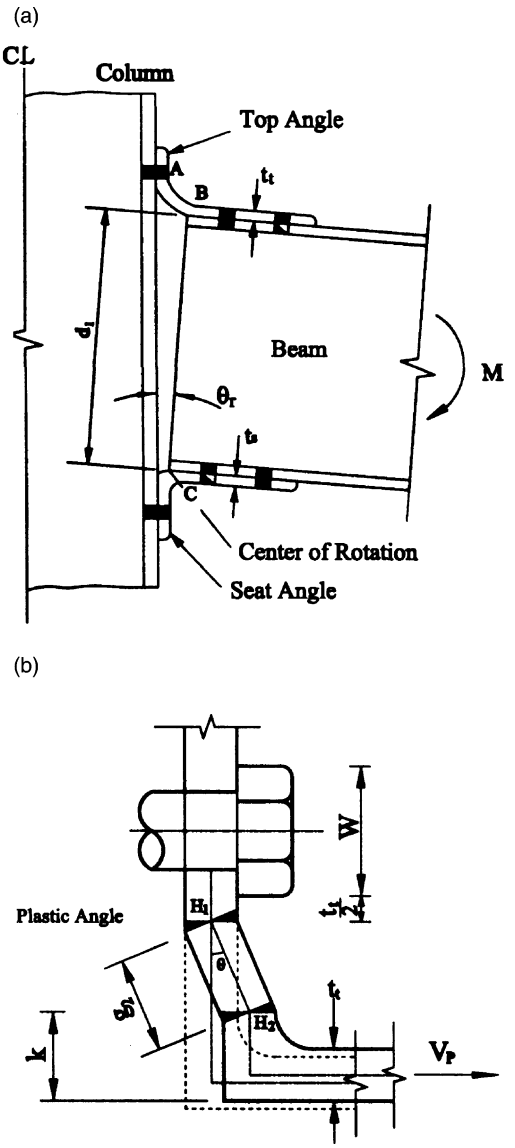

Fig. 4. Top and seat angle connection. (a) Deflected configuration at elastic condition and (b) mechanism at ultimate condition.

4. Practical advanced analysis

4.1. Geometric second-order effects

Stability functions are used to capture the second-order effects since they can account for the effect of the axial force on the bending stiffness reduction of a member. The benefit of using stability functions is that it enables only one or two elements to predict 'accurately the second-order effect of each framed member (Kim and Chen, 1996a,b).

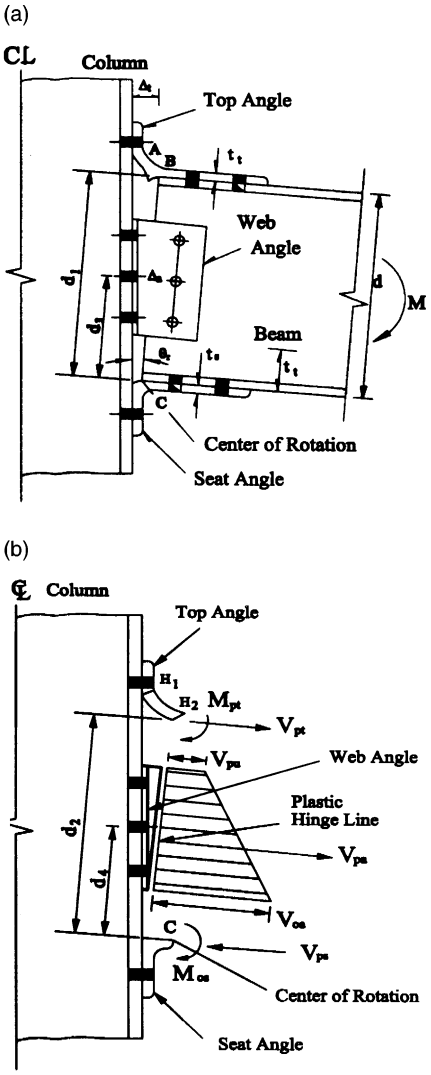

Fig. 5. Top and seat angle with web-angle connection. (a) Deflected configuration at elastic condition and (b) applied forces in ultimate state of connection.

The force–displacement equation using stability functions may be written for three-dimensional beam-column element as

$$\begin{Bmatrix} P \\ M_{yA} \\ M_{yB} \\ M_{zA} \\ M_{zB} \\ T \end{Bmatrix} = \begin{bmatrix} \frac{EA}{L} & 0 & 0 & 0 & 0 & 0 \\ 0 & S_1\frac{EI_y}{L} & S_2\frac{EI_y}{L} & 0 & 0 & 0 \\ 0 & S_2\frac{EI_y}{L} & S_1\frac{EI_y}{L} & 0 & 0 & 0 \\ 0 & 0 & 0 & S_3\frac{EI_z}{L} & S_4\frac{EI_z}{L} & 0 \\ 0 & 0 & 0 & S_4\frac{EI_z}{L} & S_3\frac{EI_z}{L} & 0 \\ 0 & 0 & 0 & 0 & 0 & \frac{GJ}{L} \end{bmatrix} \begin{Bmatrix} \delta \\ \theta_{yA} \\ \theta_{yB} \\ \theta_{zA} \\ \theta_{zB} \\ \phi \end{Bmatrix} \tag{10}$$

Table 1
Empirical equations for shape parameter n (Kishi and Chen, 1990)

Connection type	N
Single web-angle connection	$0.520\log_{10}\theta_0 + 2.291$ for $\log_{10}\theta_0 > -3.073$ 0.695 for $\log_{10}\theta_0 < -3.073$
Double web-angle connection	$1.322\log_{10}\theta_0 + 3.952$ for $\log_{10}\theta_0 > -2.582$ 0.573 for $\log_{10}\theta_0 < -2.582$
Top and seat angle connection	$2.003\log_{10}\theta_0 + 6.070$ for $\log_{10}\theta_0 > -2.880$ 0.302 for $\log_{10}\theta_0 < -2.880$
Top and seat angle connection with double web-angle	$1.398\log_{10}\theta_0 + 4.631$ for $\log_{10}\theta_0 > -2.721$ 0.827 for $\log_{10}\theta_0 < -2.721$

where P, M_{yA}, M_{yB}, M_{zA}, M_{zB}, and, T are axial force, end moments with respect to y and z axes and torsion respectively. δ, θ_{yA}, θ_{yB}, θ_{zA}, θ_{zB}, and, ϕ are the axial displacement, the joint rotations, and the angle of twist. S_1, S_2, S_3, and S_4 are the stability functions with respect to y and z axes, respectively.

The stability functions given by Eq. (10) may be written as

$$S_1 = \begin{cases} \dfrac{\pi\sqrt{\rho_y}\sin(\pi\sqrt{\rho_y}) - \pi^2\rho\cos(\pi\sqrt{\rho_y})}{2 - 2\cos(\pi\sqrt{\rho_y}) - \pi\sqrt{\rho_y}\sin(\pi\sqrt{\rho_y})} & \text{if} \quad P < 0 \\ \dfrac{\pi^2\rho_y\cosh(\pi\sqrt{\rho_y}) - \pi\sqrt{\rho_y}\sinh(\pi\sqrt{\rho_y})}{2 - 2\cosh(\pi\sqrt{\rho_y}) + \pi\sqrt{\rho_y}\sinh(\pi\sqrt{\rho_y})} & \text{if} \quad P > 0 \end{cases} \tag{11a}$$

$$S_2 = \begin{cases} \dfrac{\pi^2\rho_y - \pi\sqrt{\rho_y}\sin(\pi\sqrt{\rho_y})}{2 - 2\cos(\pi\sqrt{\rho_y}) - \pi\sqrt{\rho_y}\sin(\pi\sqrt{\rho_y})} & \text{if} \quad P < 0 \\ \dfrac{\pi\sqrt{\rho_y}\sinh(\pi\sqrt{\rho_y}) - \pi^2\rho_y}{2 - 2\cosh(\pi\sqrt{\rho_y}) + \pi\sqrt{\rho_y}\sin(\pi\sqrt{\rho_y})} & \text{if} \quad P > 0 \end{cases} \tag{11b}$$

$$S_3 = \begin{cases} \dfrac{\pi\sqrt{\rho_z}\sin(\pi\sqrt{\rho_z}) - \pi^2\rho\cos(\pi\sqrt{\rho_z})}{2 - 2\cos(\pi\sqrt{\rho_z}) - \pi\sqrt{\rho_z}\sin(\pi\sqrt{\rho_z})} & \text{if} \quad P < 0 \\ \dfrac{\pi^2\rho\cosh(\pi\sqrt{\rho_z}) - \pi\sqrt{\rho_z}\sinh(\pi\sqrt{\rho_z})}{2 - 2\cosh(\pi\sqrt{\rho_z}) + \pi\sqrt{\rho_z}\sinh(\pi\sqrt{\rho_z})} & \text{if} \quad P > 0 \end{cases} \tag{11c}$$

$$S_4 = \begin{cases} \dfrac{\pi^2\rho_z - \pi\sqrt{\rho_z}\sin(\pi\sqrt{\rho_z})}{2 - 2\cos(\pi\sqrt{\rho_z}) - \pi\sqrt{\rho_z}\sin(\pi\sqrt{\rho_z})} & \text{if} \quad P < 0 \\ \dfrac{\pi\sqrt{\rho_z}\sinh(\pi\sqrt{\rho_z}) - \pi^2\rho_z}{2 - 2\cosh(\pi\sqrt{\rho_z}) + \pi\sqrt{\rho_z}\sin(\pi\sqrt{\rho_z})} & \text{if} \quad P > 0 \end{cases} \tag{11d}$$

where $\rho_y = P/(\pi^2 EI_y/L^2)$, $\rho_z = P/(\pi^2 EI_z/L^2)$, and P is positive in tension.

4.2. Column research council tangent modulus model associated with residual stresses

The CRC tangent modulus concept is used to account for gradual yielding (due to residual stresses) along the length of axially loaded members between plastic hinges. The elastic modulus E (instead of moment of inertia I) is reduced to account for the reduction of the elastic portion of the cross-section since the reduction of the elastic modulus is easier to implement than a new moment of inertia for every different section. From Chen and Lui (1991), the CRC E_t is written as

$$E_t = 1.0E \quad \text{for } P \leqslant 0.5P_y \tag{12a}$$

$$E_t = 4\frac{P}{P_y}E\left(1 - \frac{P}{P_y}\right) \quad \text{for } P > 0.5P_y \tag{12b}$$

4.3. Parabolic function for gradual yielding due to flexure

The tangent modulus model is suitable for the member subjected to axial force, but not adequate for cases of both axial force and bending moment. A gradual stiffness degradation model for a plastic hinge is required to represent the partial plastification effects associated with bending. We shall introduce the parabolic function to represent the transition from elastic to zero stiffness associated with a developing hinge. When the parabolic function for a gradual yielding is active at both ends of an element, the slope-deflection equation may be expressed as

$$\begin{Bmatrix} P \\ M_{yA} \\ M_{yB} \\ M_{zA} \\ M_{zB} \\ T \end{Bmatrix} = \begin{bmatrix} \frac{E_tA}{L} & 0 & 0 & 0 & 0 & 0 \\ 0 & k_{iiy} & k_{ijy} & 0 & 0 & 0 \\ 0 & k_{ijy} & k_{jjy} & 0 & 0 & 0 \\ 0 & 0 & 0 & k_{iiz} & k_{ijz} & 0 \\ 0 & 0 & 0 & k_{ijz} & k_{jjz} & 0 \\ 0 & 0 & 0 & 0 & 0 & \frac{GJ}{L} \end{bmatrix} \begin{Bmatrix} \delta \\ \theta_{yA} \\ \theta_{yB} \\ \theta_{zA} \\ \theta_{zB} \\ \phi \end{Bmatrix} \tag{13}$$

where

$$k_{iiy} = \eta_A\left(S_1 - \frac{S_2^2}{S_1}(1 - \eta_B)\right)\frac{E_tI_y}{L} \tag{14a}$$

$$k_{ijy} = \eta_A\eta_B S_2\frac{E_tI_y}{L} \tag{14b}$$

$$k_{jjy} = \eta_B\left(S_1 - \frac{S_2^2}{S_1}(1 - \eta_A)\right)\frac{E_tI_y}{L} \tag{14c}$$

$$k_{iiz} = \eta_A\left(S_3 - \frac{S_4^2}{S_3}(1 - \eta_B)\right)\frac{E_tI_z}{L} \tag{14d}$$

$$k_{ijz} = \eta_A\eta_B S_4\frac{E_tI_z}{L} \tag{14e}$$

$$k_{jjz} = \eta_B\left(S_3 - \frac{S_4^2}{S_3}(1 - \eta_A)\right)\frac{E_tI_z}{L} \tag{14f}$$

The terms η_A and η_B is a scalar parameter that allows for gradual inelastic stiffness reduction of the element associated with plastification at end A and B. This term is equal to 1.0 when the element is elastic, and zero when a plastic hinge is formed. The parameter η is assumed to vary according to the parabolic function:

$$\eta = 1.0 \quad \text{for } \alpha \leqslant 0.5 \tag{15a}$$

$$\eta = 4\alpha(1 - \alpha) \quad \text{for } \alpha > 0.5 \tag{15b}$$

where α is a force-state parameter that measures the magnitude of axial force and bending moment at the element end. The term (α) may be expressed by AISC-LRFD and Orbison, respectively:

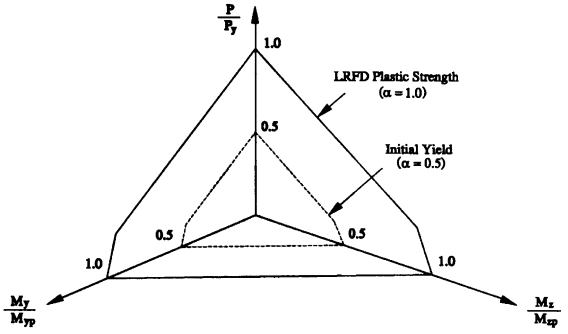

Fig. 6. Full plastification surface of AISC-LRFD.

AISC-LRFD

Based AISC-LRFD bilinear interaction equation (Kanchanalai, 1977), the cross-section plastic strength of the beam-column member may be expressed (Fig. 6)

$$\alpha = \frac{P}{P_y} + \frac{8}{9}\frac{M_y}{M_{yp}} + \frac{8}{9}\frac{M_z}{M_{zp}} \qquad \text{for} \quad \frac{P}{P_y} \geqslant \frac{2}{9}\frac{M_y}{M_{yp}} + \frac{2}{9}\frac{M_z}{M_{zp}} \tag{16a}$$

$$\alpha = \frac{P}{2P_y} + \frac{M_y}{M_{yp}} + \frac{M_z}{M_{zp}} \qquad \text{for} \quad \frac{P}{P_y} < \frac{2}{9}\frac{M_y}{M_{yp}} + \frac{2}{9}\frac{M_z}{M_{zp}} \tag{16b}$$

Orbison

Orbison's full plastification surface (Fig. 7) (Orbison, 1982) of cross-section is given by

$$\alpha = 1.15p^2 + m_z^2 + m_y^4 + 3.67p^2m_z^2 + 3.0p^6m_y^2 + 4.65m_z^4m_y^2 \tag{17}$$

where, $p = P/P_y$, $m_z = M_z/M_{pz}$ (strong axis), $m_y = M_y/M_{py}$ (weak axis).

4.4. Shear deformation

The stiffness coefficients should be modified to account for the effect of the additional flexural shear deformation in a beam-column element. The flexural flexibility matrix can be obtained by inversing the flexural stiffness matrix as

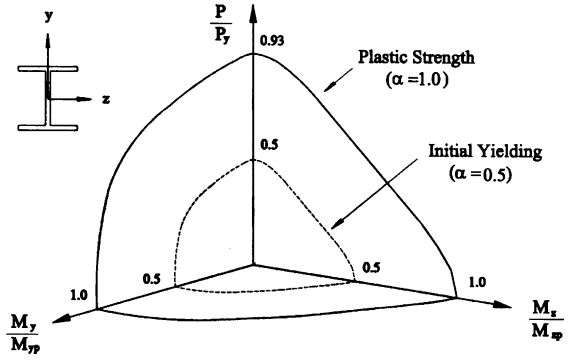

Fig. 7. Full plastification surface of Orbison.

$$\begin{Bmatrix} \theta_{MA} \\ \theta_{MB} \end{Bmatrix} = \begin{bmatrix} \frac{k_{jj}}{k_{ii}k_{jj}-k_{ij}^2} & -\frac{k_{ij}}{k_{ii}k_{jj}-k_{ij}^2} \\ -\frac{k_{ij}}{k_{ii}k_{jj}-k_{ij}^2} & \frac{k_{ii}}{k_{ii}k_{jj}-k_{ij}^2} \end{bmatrix} \begin{Bmatrix} M_{\mathrm{A}} \\ M_{\mathrm{B}} \end{Bmatrix} \tag{18}$$

where k_{ii}, k_{ij}, and k_{jj} are the elements of stiffness matrix in a planar beam-column. θ_{MA} and θ_{MB} are the slope of the neutral axis due to bending moment. The flexibility matrix corresponding to flexural shear deformation may be written as

$$\begin{Bmatrix} \theta_{SA} \\ \theta_{SB} \end{Bmatrix} = \begin{bmatrix} \frac{1}{GA_sL} & \frac{1}{GA_sL} \\ \frac{1}{GA_sL} & \frac{1}{GA_sL} \end{bmatrix} \begin{Bmatrix} M_{\mathrm{A}} \\ M_{\mathrm{B}} \end{Bmatrix} \tag{19}$$

where GA_s and L are shear rigidity and length of the beam-column, respectively. Total rotation at the A and B is obtained by combining Eqs. (18) and (19) as

$$\begin{Bmatrix} \theta_{\mathrm{A}} \\ \theta_{\mathrm{B}} \end{Bmatrix} = \begin{Bmatrix} \theta_{MA} \\ \theta_{MB} \end{Bmatrix} + \begin{Bmatrix} \theta_{SA} \\ \theta_{SB} \end{Bmatrix} \tag{20}$$

The force–displacement equation including flexural shear deformation is obtained by inversing the flexibility matrix as

$$\begin{Bmatrix} M_{\mathrm{A}} \\ M_{\mathrm{B}} \end{Bmatrix} = \begin{bmatrix} \frac{k_{ii}k_{jj}-k_{ij}^2+k_{ii}A_sGL}{k_{ii}+k_{jj}+2k_{ij}+A_sGL} & \frac{-k_{ii}k_{jj}+k_{ij}^2+k_{ij}A_sGL}{k_{ii}+k_{jj}+2k_{ij}+A_sGL} \\ \frac{-k_{ii}k_{jj}+k_{ij}^2+k_{ij}A_sGL}{k_{ii}+k_{jj}+2k_{ij}+A_sGL} & \frac{k_{ii}k_{jj}-k_{ij}^2+k_{ij}A_sGL}{k_{ii}+k_{jj}+2k_{ij}+A_sGL} \end{bmatrix} \begin{Bmatrix} \theta_{\mathrm{A}} \\ \theta_{\mathrm{B}} \end{Bmatrix} \tag{21}$$

The force–displacement equation may be written for three-dimensional beam-column element as

$$\begin{Bmatrix} P \\ M_{yA} \\ M_{yB} \\ M_{zA} \\ M_{zB} \\ T \end{Bmatrix} = \begin{bmatrix} \frac{E_tA}{L} & 0 & 0 & 0 & 0 & 0 \\ 0 & C_{iiy} & C_{ijy} & 0 & 0 & 0 \\ 0 & C_{ijy} & C_{jjy} & 0 & 0 & 0 \\ 0 & 0 & 0 & C_{iiz} & C_{ijz} & 0 \\ 0 & 0 & 0 & C_{ijz} & C_{jjz} & 0 \\ 0 & 0 & 0 & 0 & 0 & \frac{GJ}{L} \end{bmatrix} \begin{Bmatrix} \delta \\ \theta_{yA} \\ \theta_{yB} \\ \theta_{zA} \\ \theta_{zB} \\ \phi \end{Bmatrix} \tag{22}$$

in which

$$C_{iiy} = \frac{k_{iiy}k_{jjy}-k_{ijy}^2+k_{iiy}A_{sz}GL}{k_{iiy}+k_{jjy}+2k_{ijy}+A_{sz}GL} \tag{23a}$$

$$C_{ijy} = \frac{-k_{iiy}k_{jjy}+k_{ijy}^2+k_{ijy}A_{sz}GL}{k_{iiy}+k_{jjy}+2k_{ijy}+A_{sz}GL} \tag{23b}$$

$$C_{jjy} = \frac{k_{iiy}k_{jjy}-k_{ijy}^2+k_{jjy}A_{sz}GL}{k_{iiy}+k_{jjy}+2k_{ijy}+A_{sz}GL} \tag{23c}$$

$$C_{iiz} = \frac{k_{iiz}k_{jjz}-k_{ijz}^2+k_{iiz}A_{sy}GL}{k_{iiz}+k_{jjz}+2k_{ijz}+A_{sy}GL} \tag{23d}$$

$$C_{ijz} = \frac{-k_{iiz}k_{jjz}+k_{ijz}^2+k_{ijz}A_{sy}GL}{k_{iiz}+k_{jjz}+2k_{ijz}+A_{sy}GL} \tag{23e}$$

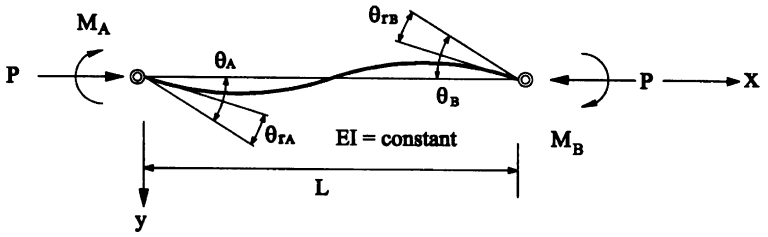

Fig. 8. Beam-column element with semi-rigid connections.

$$C_{jjz} = \frac{k_{iiz}k_{jjz} - k_{ijz}^2 + k_{jjz}A_{sy}GL}{k_{iiz} + k_{jjz} + 2k_{ijz} + A_{sy}GL} \tag{23f}$$

where A_{sy} and A_{sz} are the effective shear flexure shear areas with respect to y and z axes, respectively.

4.5. Effect of semi-rigid connection

The connection may be modeled as a rotational spring in the moment–rotation relationship represented by Eq. (22). Fig. 8 shows a beam-column element with semi-rigid connections at both ends. If the effect of connection flexibility is incorporated into the member stiffness, the incremental element force–displacement relationship of Eq. (22) is modified as

$$\begin{Bmatrix} P \\ M_{yA} \\ M_{yB} \\ M_{zA} \\ M_{zB} \\ T \end{Bmatrix} = \begin{bmatrix} \frac{E_t A}{L} & 0 & 0 & 0 & 0 & 0 \\ 0 & C_{iiy}^* & C_{ijy}^* & 0 & 0 & 0 \\ 0 & C_{ijy}^* & C_{jjy}^* & 0 & 0 & 0 \\ 0 & 0 & 0 & C_{iiz}^* & C_{ijz}^* & 0 \\ 0 & 0 & 0 & C_{ijz}^* & C_{jjz}^* & 0 \\ 0 & 0 & 0 & 0 & 0 & \frac{GJ}{L} \end{bmatrix} \begin{Bmatrix} \delta \\ \theta_{yA} \\ \theta_{yB} \\ \theta_{zA} \\ \theta_{zB} \\ \phi \end{Bmatrix} \tag{24}$$

where

$$C_{iiy}^* = \frac{\left(C_{iiy} + \frac{C_{iiy}C_{jjy}}{R_{ktYB}} - \frac{C_{ijy}^2}{R_{ktYB}}\right)}{R_Y^*} \tag{25a}$$

$$C_{jjy}^* = \frac{\left(C_{jjy} + \frac{C_{iiy}C_{jjy}}{R_{ktYA}} - \frac{C_{ijy}^2}{R_{ktYA}}\right)}{R_Y^*} \tag{25b}$$

$$C_{ijy}^* = \frac{C_{ijy}}{R_Y^*} \tag{25c}$$

$$C_{iiz}^* = \frac{\left(C_{iiz} + \frac{C_{iiz}C_{jjz}}{R_{ktZB}} - \frac{C_{ijz}^2}{R_{ktZB}}\right)}{R_Z^*} \tag{25d}$$

$$C_{jjz}^* = \frac{\left(C_{jjz} + \frac{C_{iiz}C_{jjz}}{R_{ktZA}} - \frac{C_{ijz}^2}{R_{ktZA}}\right)}{R_Z^*} \tag{25e}$$

$$C^*_{ijz} = \frac{C_{ijz}}{R^*_Z} \tag{25f}$$

$$R^*_Y = \left(1 + \frac{C_{iiy}}{R_{ktYA}}\right)\left(1 + \frac{C_{jjy}}{R_{ktYB}}\right) - \frac{C^2_{ijy}}{R_{ktYA}R_{ktYB}} \tag{25g}$$

$$R^*_Z = \left(1 + \frac{C_{iiz}}{R_{ktZA}}\right)\left(1 + \frac{C_{jjz}}{R_{ktZB}}\right) - \frac{C^2_{ijz}}{R_{ktZA}R_{ktZB}} \tag{25h}$$

in which R_{ktYA} = tangent stiffness of connections A in the Y-direction, R_{ktYB} = tangent stiffness of connections B in the Y-direction, R_{ktZA} = tangent stiffness of connections A in the Z-direction, and R_{ktZB} = tangent stiffness of connections B in the Z-direction.

5. Verification study

In the open literature, no available benchmark problems of semi-rigid space frames are available for verification study. One way to verify the proposed analysis is to make separate verifications for the effects of semi-rigid connections of a planar frame and for the nonlinear behavior of the column and the space rigid frame.

5.1. Effect of semi-rigid connections of a planar frame

Stelmack (1982) studied the experimental response of two flexibly connected steel frames. A two-story, one-bay frame among his study is selected as a benchmark frame in the present study. The benchmark frame was fabricated from the same A36 W5 × 16 sections, and all column bases are pinned supports in Fig. 9. The connections used in the frame were bolted top and seat angles connections of L4 × 4 × 1/2 made of A36 with bolt fasteners of A325 3/4-in. D, and its experimental moment–rotation relationship is shown in Fig. 10. Gravity loading of 10.7 kN (2.4 kips) was first applied at third points of the beam of the first floor, and then a lateral load was applied as the second loading sequence. The lateral load–displacement relationship was provided by the experimental work.

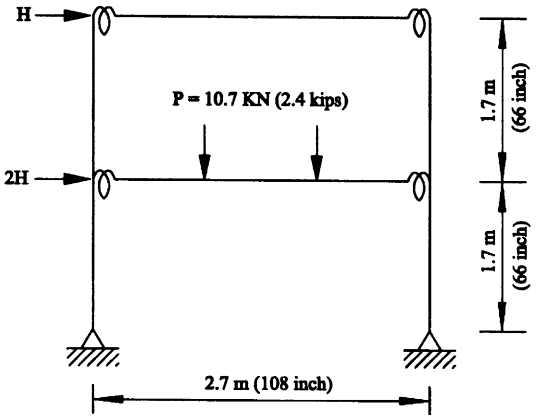

Fig. 9. Configuration and load condition of Stelmack's two-story semi-rigid frame.

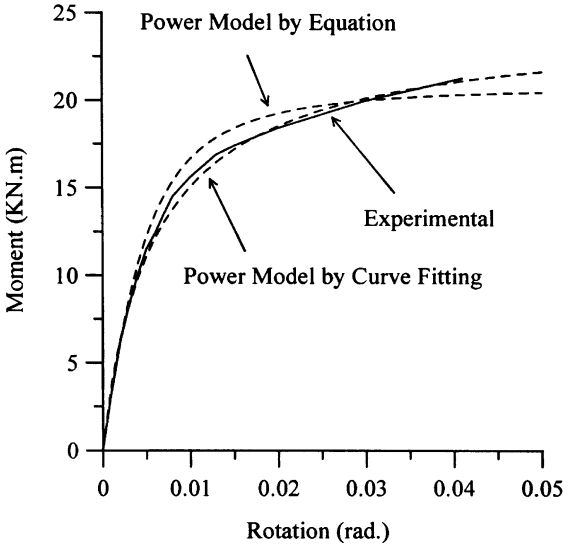

Fig. 10. Comparison of moment–rotation behavior by experiment and three-parameter power model for verification study.

Herein, the three parameters of the power model are determined by a curve-fitting and Eqs. (4)–(9) combined with Table 1. The curves by the experiment and by the curve-fitting result in a good agreement as shown in Fig. 10. The parameters by Kishi–Chen equations and by the experiment show a difference to some degree as shown in Table 2 and Fig. 10. In spite of this difference, Kishi–Chen equations are preferably in practical design since experimental moment–rotation curves are not available in design stages, in general. In the analysis, the gravity load is first applied, followed by the lateral load. The lateral displacements by the proposed methods and by the experiment compare well in Fig. 11. As a result, the proposed analysis is adequate in predicting the behavior and strength of semi-rigid connections.

5.2. Column with three-dimensional degree of freedom

A simply supported column with three-dimensional degree of freedom is shown in Fig. 12. W8 × 31 column of A36 steel is used for the analysis. The column strength calculated by the proposed analysis, Euler solution, and DRAIN-3DX based on the slenderness parameter λ_c are compared in Fig. 13.

The strength of the proposed analysis compares well with Euler's theoretical solution. The maximum error from the proposed analysis is 1.31% for the practical range of columns ($\lambda_c \leqslant 2.0$). However, DRAIN-3DX produces the maximum error of 21.16%. The large error value is a result of not considering the interaction of the axial force and bending moments when considering geometric nonlinear effect.

Table 2
Comparison of the three parameters of power model for verification

Parameters	Curve-fitting	Kishi–Chen
Initial stiffness	4,520 kN-m/rad (40,000 kip-in/rad)	3,374 kN-m/rad (29,855 kip-in/rad)
Ultimate moment	24.9 kN-m/rad (220 kip-in/rad)	20.9 kN-m/rad (185 kip-in/rad)
Shape parameter	0.91	1.65

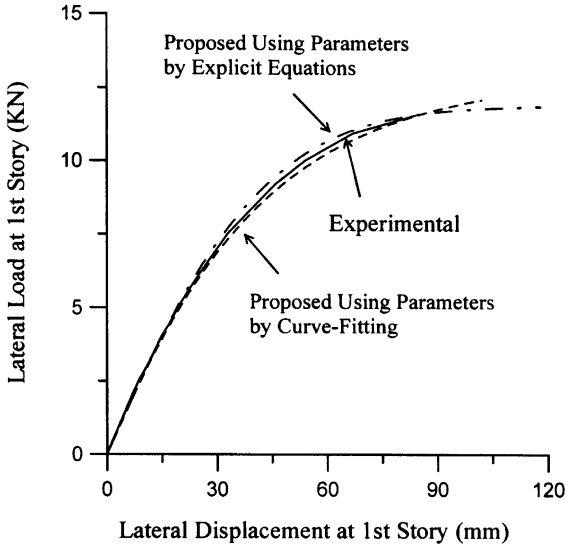

Fig. 11. Comparison of lateral displacements by experiment and proposed methods for verification study.

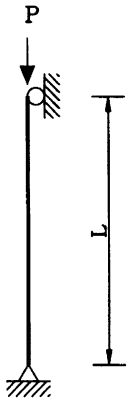

Fig. 12. Column.

5.3. Nonlinear behavior of space rigid frame

Fig. 14 shows Orbison's six-story space frame (Orbison, 1982). The yield strength of all members is 250 MPa (36 ksi) and Young's modulus is 206,850 MPa (30,000 ksi). Uniform floor pressure of 4.8 kN/m^2 (100 psf) is converted into equivalent concentrated loads on the top of the columns. Wind loads are simulated by point loads of 26.7 kN (6 kips) in the Y-direction at every beam-column joints.

The load–displacement results calculated by the proposed analysis compare well with those of Liew and Tang's (considering shear deformations) and Orbison's (ignoring shear deformations) results (Tables 3 and 4, and Fig. 15). The ratios of load carrying capacities (calculated from the proposed analysis) over the applied loads are 2.057 and 2.066. These values are nearly equivalent to 2.062 and 2.059 calculated by Liew and Tang and Orbison, respectively.

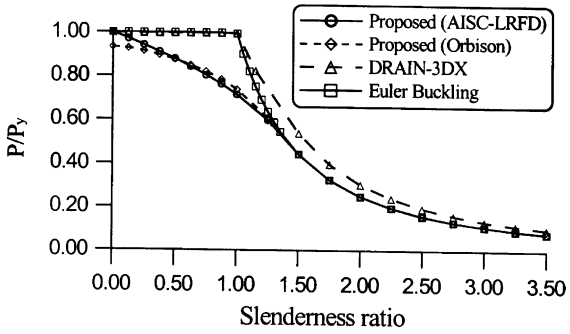

Fig. 13. Comparison of column strength.

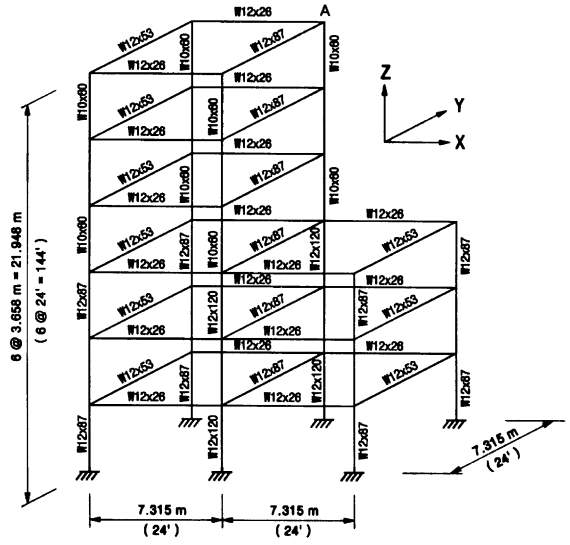

Fig. 14. Space frame of six-story.

Table 3
Result of analysis considering shear deformation

Method	Proposed		Liew's
Plastic strength surface	LRFD	Orbison	Orbison
Ultimate load factor	1.990	2.057	2.062
Displacement at A in Y-direction (mm)	208	219	250

Table 4
Result of analysis ignoring shear deformation

Method	Proposed		Orbison's
Plastic strength surface	LRFD	Orbison	Orbison
Ultimate load factor	1.997	2.066	2.059
Displacement at A in Y-direction (mm)	199	208	247

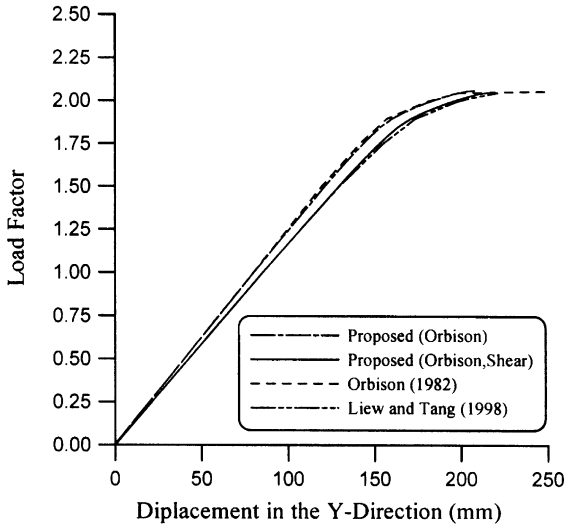

Fig. 15. Comparison of load–displacement of six-story space frame.

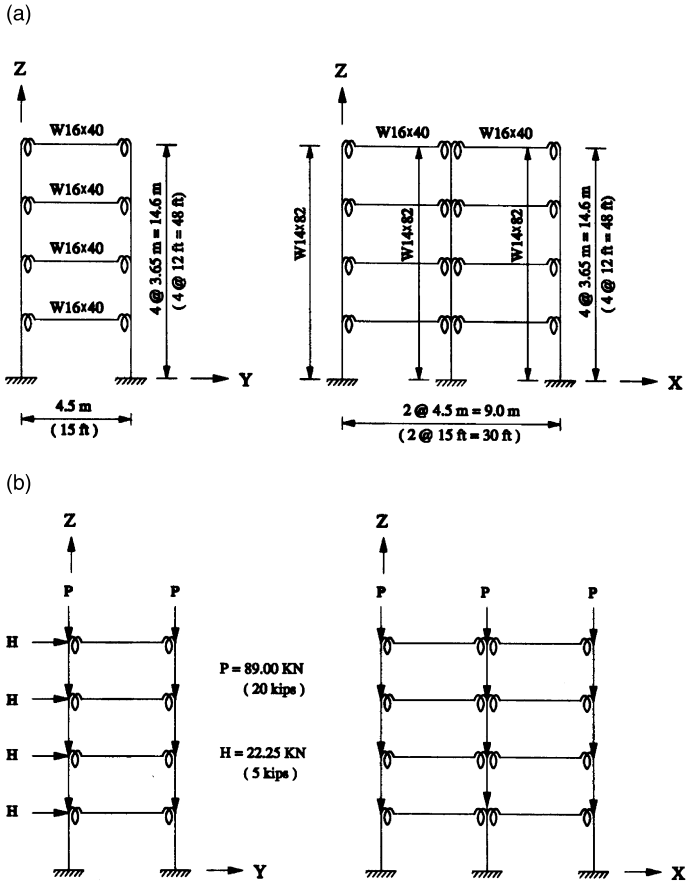

Fig. 16. Three-dimensional semi-rigid frame. (a) Configuration and (b) load case.

Table 5
Parameter for connection

Initial stiffness	Ultimate moment	Shape parameter
63,148 kN-m/rad (557,858 k-in/rad)	107 kN-m/rad (950 kip-in/rad)	0.524

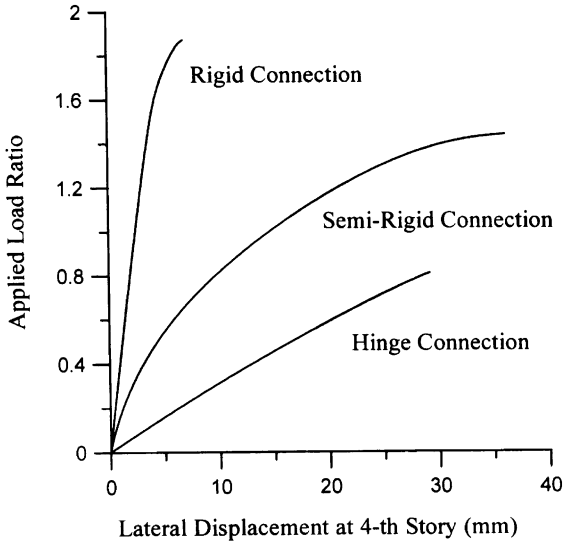

Fig. 17. Load–displacement relationship.

6. Case study

Fig. 16 shows a four-story semi-rigid frame. Each story was 3.65 m (12 ft) high and 4.5 m (15 ft) wide. The frame was subjected to concentrated gravity and lateral loads. The members were W14 × 82 for the column and W16 × 40 the beam. The yield strength of all member was 248 MPa (36 ksi) and Young's modulus was 206,850 MPa (30,000 ksi). The beam connections were top- and seat-angles of L6 × 4 × 9/16 × 7. All fasteners were A325 3/5-in. Diameter bolts. Three parameters computed are given in Table 5. The load–displacement curves of semi-rigid, rigid, and hinged connection are compared in Fig. 17. The rigid, semi-rigid, and hinged frame collapse when the applied load ratio reached 1.87, 1.45, and 0.81, respectively. Thus, semi-rigid connection is a very crucial element to be considered in advanced analysis.

7. Conclusions

In this paper, a practical advanced analysis of three-dimensional semi-rigid frames has been developed by combining nonlinear behavior of framed members and that of semi-rigid connection. The conclusions of this study are as follows:

1. The proposed methods can predict accurately the combined effects of connection, geometric, and material nonlinearities for semi-rigid frames.
2. The practical procedures for determining connection parameters are provided for a given connection configuration.

3. Stability functions enable only one or two element per member to capture second-order effects that make the proposed analysis practical.
4. The CRC tangent modulus and a parabolic function consisting of member forces for gradual yielding predict inelastic behavior reasonably well.
5. The strengths predicted by these methods are compared well those available experiments.
6. In the case study, the rigid, semi-rigid, and hinged frame collapse when the applied load ratio reached 1.87, 1.45, and 0.81, respectively. Thus, semi-rigid connection is a very crucial element to be considered in advanced analysis.
7. The proposed analysis can be used in lieu of the costly plastic zone analysis.

Acknowledgements

This work presented in this paper was supported by funds of National Research Laboratory Program (2000-N-NL-01-C-162) from Ministry of Science & Technology in Korea. Authors wish to appreciate the financial support.

References

Al-Mashary, F., Chen, W.F., 1991. Simplified second-order inelastic analysis for steel frames. Struct. Engng. 69, 395–399.

American Institute of Steel Construction, 1993. Manual of steel construction, load and resistance factor design, second ed., vols. 1 and 2, Chicago, IL.

Barsan, G.M., Chiorean, C.G., 1999. Computer program for large deflection elasto-plastic analysis of semi-rigid steel frameworks. Comput. Struct. 72, 699–711.

Chen, W.F., Kishi, N., 1989. Semi-rigid steel beam-to-column connections: data base and modeling. ASCE J. Struct. Engng. 115 (1), 105–119.

Chen, W.F., Lui, E.M., 1991. Stability Design of Steel Frames, CRC Press, Boca Raton, FL.

Chen, W.F., Toma, S., 1994. Advanced Analysis of Steel Frames, CRC Press, Boca Raton, FL.

Goverdhan, A.V., 1983. A collection of experimental moment–rotation Curves and evaluation of prediction equations for semi-rigid connections. Mater's Thesis, Vanderbilt University, Nashville, TN, 490.

Kanchanalai, T., 1977. The design and behavior of beam-columns in unbraced steel frames, AISI Project no. 189, report no. 2, Civil Engineering/structures Research Lab., University of Texas, Austin, TX, 300.

Kim, S.E., Chen, W.F., 1996a. Practical advanced analysis for braced steel frame design. ASCE J. Struct. Engng. 122 (11), 1266–1274.

Kim, S.E., Chen, W.F., 1996b. Practical advanced analysis for unbraced steel frame design. ASCE J. Struct. Engng. 122 (11), 1259–1265.

Kishi, N., Chen, W.F., 1986. Data base of steel beam-to-column connections, Structural Engineering Report no. CE-STR-86-26, School of Civil Engineering, Purdue University, West Lafayette, IN, 653.

Kish, N., Chen, W.F., 1990. Moment-rotation relations of semi-rigid connections with angles. ASCE J. Struct. Engng. 116 (7), 1813–1834.

Kishi, N., Chen, W.F., Goto, Y., Matsuoka K.G., 1991. Applicability of three-parameter power model to structural analysis of flexibly jointed frames, Proc. Mechanics Computing in 1990's and Beyond, Columbus, OH, 233–237.

Liew, J.Y.R., 1992. Advanced analysis for frame design, Ph.D. Thesis, School of Civil Engineering, Purdue University, West Lafayette, IN, 392.

Liew, J.Y.R., Tang, L.K., 1998. Nonlinear refined plastic hinge analysis of space frame structures, Research Report no. CE027/98, Department of Civil Engineering, National University of Singapore, Singapore.

Lui, E.M., Chen, W.F., 1986. Analysis and behavior of flexibly jointed frames. Engng. Struct. 8, 107–118.

Nethercot, D.A., 1985. Steel beam-to-column connections – a review of test data and its applicability to the evaluation of joint behavior in the performance of steel frames, CIRIA Project Record, RP 338.

Orbison, J.G., 1982. Nonlinear static analysis of three-dimensional steel frames, Report no. 82-6, Department of Structural Engineering, Cornell University, Ithaca, New York.

Prakash, V., Powell, G.H., 1993. DRAIN-3DX: Base program user guide, version 1.10, A Computer Program Distributed by NISEE/Computer Applications, Department of Civil Engineering, University of California, Berkeley.

Shakourzadeh, H., Guo, Y.Q., Bato, J.L., 1999. Modeling of connections in the analyses of thin-walled space frames. Comput. Struct. 71, 423–433.

Stelmack, T.W., 1982. Analytical and experimental response of flexibly-connected steel frames, M.S. Thesis, Department of Civil Environmental and Architectural Engineering, University of Colorado, 134.